Available online at www.sciencedirect.com
ScienceDirect
Journal of Power Sources 162 (2006) 492–496
JOURNAL OF POWER SOURCES
www.elsevier.com/locate/jpowsour

Short communication

Template preparation of Pt–Ru and Pt nanowire array electrodes on a Ti/Si substrate for methanol electro-oxidation

Guang-Yu Zhao, Cai-Ling Xu, Dao-Jun Guo, Hua Li, Hu-Lin Li *

College of Chemistry and Chemical Engineering, Lanzhou University, Lanzhou 730000, PR China

Received 3 April 2006; received in revised form 28 June 2006; accepted 29 June 2006
Available online 4 August 2006

Abstract

Pt and Pt–Ru nanowire array electrodes were obtained by dc (direct current) electrodeposition of Pt and Ru into the pores of an anodic aluminum oxide (AAO) template on a Ti/Si substrate. Transmission electron microscope (TEM) examination showed all the nanowires had a uniform diameter of about 30 nm. The brush shaped Pt and Pt–Ru nanowire array electrodes could be seen clearly by scanning electron microscope. Pt and Pt–Ru nanowire array electrodes gave the X-ray diffraction pattern of a face-centered cubic (fcc) crystal structure. The electro-oxidation of methanol on these electrodes was investigated at room temperature using cyclic voltammetry. The results demonstrated that the alloy nanowire array electrode was catalytically more active than a pure platinum nanowire array electrode and the Pt–Ru nanowire array electrode may have good potential for applications in portable fuel cell power sources.

Keywords: Portable power sources; AAO/Ti/Si; Pt and Pt–Ru nanowire array electrodes; Electro-catalysis; Methanol oxidation

1. Introduction

Portable power sources are critical for mobile devices such as celluller phones, lap top computers, pacemakers, and various microsystems. Direct methanol fuel cells (DMFC) are attractive as portable power sources [1–7] because they require only the introduction of methanol to generate power. They do not require the electrical charging of a traditional secondary battery. The fundamentals of the DMFC system have been studied extensively [8–12]. Several groups have made micro fuel cells using micro-fabrication technologies using C/Si plane substrates [13–18].

Research indicates that the electrochemical characteristics of the electrode materials are highly dependent on the grain size, texture, surface area and morphology. An ordered, high surface area structure of electrode materials can enhance electrochemical characteristics. Seong Ihl Woo and coworkers have demonstrated that a high surface area nanowire array electrode of the catalyst has significantly improved its capability compared with a catalyst black electrode [19]. An anodic aluminum oxide (AAO) template offers a promising route to make a high surface area, ordered nanowire electrode. Recently, PtNi nanorods for methanol electro-oxidation were prepared by the AAO template method [20]. But this method is difficult to use in practice due to the fragility of the AAO template [21–27].

In this work, AAO films were successfully grown on a Ti/Si substrate and this is the first time it was used as a template to synthesize a high surface area and ordered nanowire array electrode for methanol electro-oxidation. The electrochemical characterization of an ordered nanowire array on the Ti/Si substrate was performed by cyclic voltammetry in an 0.5 M CH_3OH + 0.5 M H_2SO_4 aqueous solution using the nanowire array as the working electrode. The electro-catalytic activity of the nanowire array electrode for methanol oxidation was investigated. The nanowire array electrode consisted of only electrochemically active material (Pt and Pt–Ru) and was fairly stable. The results demonstrate that the nanowire array electrode could have good potential applications in portable fuel cell power sources since the alloy nanowire array electrode was catalytically more active than a pure platinum nanowire array electrode.

* Corresponding author. Tel.: +86 931 891 2517; fax: +86 931 891 2582.
E-mail addresses: lihl@lzu.edu.cn, zhaogy03@st.lzu.edu.cn (H.-L. Li).

0378-7753/$ – see front matter © 2006 Elsevier B.V. All rights reserved.
doi:10.1016/j.jpowsour.2006.06.082

2. Experiments

2.1. Preparation of AAO/Ti/Si

A highly pure Al film (99.999%, ~3.5 μm) was deposited on a p-type silicon substrate coated with a Ti (~300 nm) film using radio frequency (RF) sputtering. The anodization was carried out in a 0.3 M oxalic acid solution at 20 V and room temperature for 1 h for pores of ~30 nm in diameter. The resulting aluminum film was etched away in 0.4 M H_3PO_4, 0.2 M $H_2Cr_2O_4$ at 50 °C for 2 h, and the remaining aluminum was re-anodized under the same conditions until the Al film was fully oxidized. To remove the barrier layer, the anodization was continuously processed for 30–60 min.

2.2. Preparation of the nanowire array electrodes

The electrolyte used for Pt nanowires electrodeposition was 5 mM H_2PtCl_6 and 1.2 mM HCl. The electrolyte used for the Pt–Ru nanowire electrodeposition was composed of 5 mM H_2PtCl_6, 1 mM $RuCl_3$ and 1.2 mM HCl. Electrodeposition was carried out at room temperature, using a three-electrode potentiostatic control and direct current electrodeposition system with a saturated calomel electrode (SCE) as the reference electrode. A 1.0 cm × 1.0 cm platinum plate was the counter electrode and the AAO/Ti/Si structure was the working electrode. The electrodeposition was carried out at 0 V (versus SCE) for Pt and −0.2 V (versus SCE) for Pt–Ru nanowires with a CHI 660 electrochemical analyzer. The electrodeposition was continued until the deposited nanowires "overflowed" from the nanoholes. The overflowed nanowires were mechanically polished with a metallographic abrasive paper. The as-prepared samples were immersed in 1 M NaOH for 0.5 h to remove the AAO film. Then the brush shaped nanowire array was obtained. The procedure is shown in Fig. 1.

2.3. Measurements

A conventional cell with a three-electrode configuration was used throughout this work. The nanowire array electrodes were employed as the working electrodes and a saturated calomel electrode (SCE) was used as the reference electrode. The quantity of electrocatalyst on the working electrode was 1 mg cm^{-2} which was calculated from the electrodeposition charge in Coulombs. Electrochemical measurements were performed with a CHI 660 electrochemical analyzer, and the potentials were measured with respect to SCE.

The morphology of the nanowires was characterized using a Hitachi 600 transmission electro microscope (TEM). The TEM samples were prepared by scraping the Pt and Pt–Ru nanowires from the substrate and into a vessel for dispersing in ethanol. X-ray diffraction (XRD) data of the samples were collected using a Rigaku D/MAX 24,000 diffractometer with Cu Kα radiation. The morphology of the Pt and Pt–Ru nanowire array electrodes on Ti/Si substrate were examined by scanning electron microscope (FESEM, JEOL JSM-S4800).

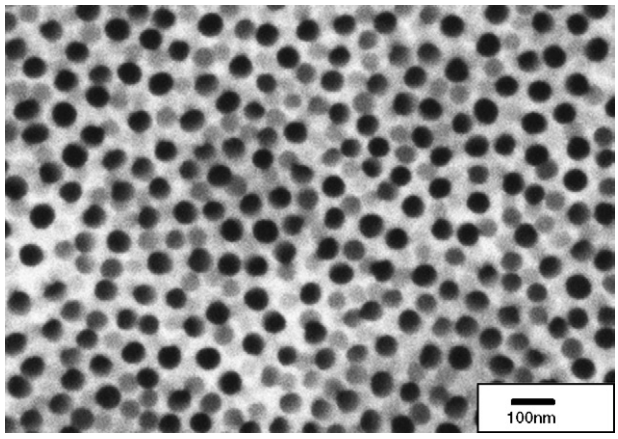

Fig. 2. FESEM images of the surface morphology of an AAO film on a Ti/Si substrate after the second anodization.

3. Results and discussion

3.1. FESEM analysis of AAO film on Ti/Si substrate

After a two-step anodization in 0.3 M oxalic acid solution at room temperature, the resulting template has parallel pores with a fairly narrow size distribution, as shown in Fig. 2. Fig. 2 shows that the porous alumina structure has an average pore diameter about 40 nm, the interspaces were about 60 nm and the pore densities about 10^{10} cm^{-2}. But their arrangement had a lower order than AAO on bulk Al probably due to the small grain size [28] and thin aluminum films [29].

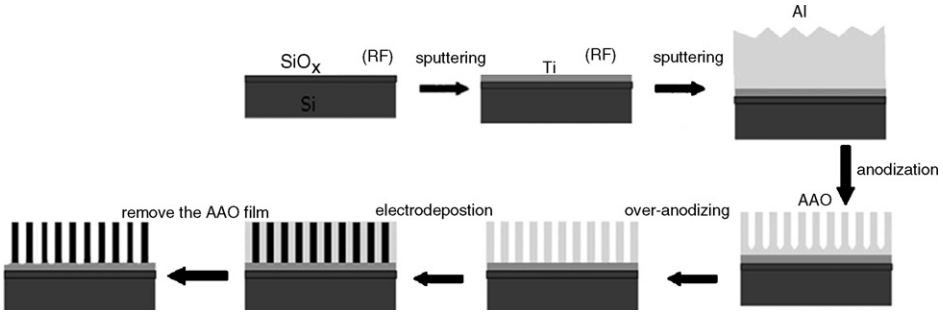

Fig. 1. Schematic of the procedure.

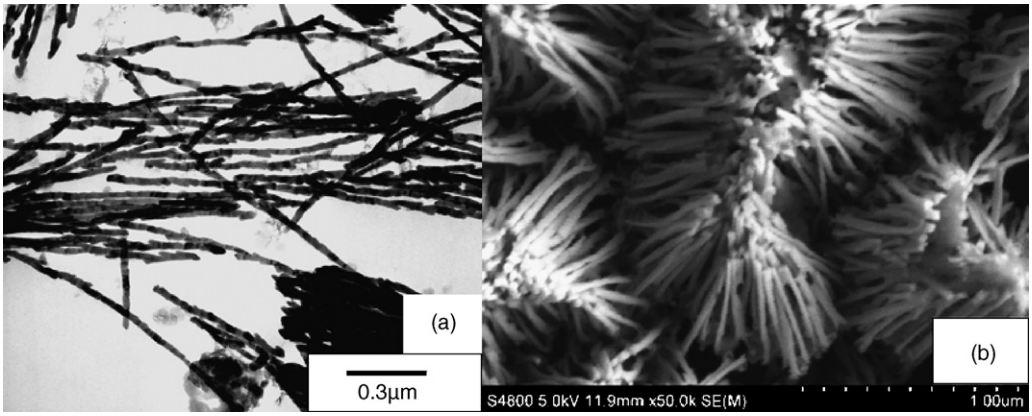

Fig. 3. TEM (a) image of the sample Pt–Ru nanowires and SEM (b) image of the surface morphology of Pt–Ru nanowire array electrode.

3.2. TEM and SEM analysis of the Pt–Ru nanowire array electrode

Fig. 3(a) shows a typical TEM image of the Pt–Ru nanowires. The TEM images reveal that the nanowires obtained on the Ti/Si substrate are of regular size and are continuous. All of them had a uniform diameter of about 30 nm, which basically was that of the pores of the AAO template used. The length of the nanowires was about 1 μm, which is identical to the thickness of the AAO template on the Ti/Si substrate. The SEM image in Fig. 3(b) shows the surface view of Pt–Ru nanowire array electrode. From Fig. 3(b), we can find that many clusters protrude from the Ti/Si substrate which provide a high surface area electrode. The clusters could result from the situation in which the nanowires are uncovered from the framework of the porous anodic aluminum template but incompletely freestanding. When the porous anodic alumina template is dissolved away, the nanowires are embedded in the template and are released gradually and inclined to agglomerate together to minimize the system free energy. Fig. 3(b) also shows that the nanowires are abundant, uniform and well ordered in the large area. From Fig. 3(b), it can be estimated that the pore filling rate is above 90%, and some nanowires are lost from the electrode surface. From the diameter, the filling rate and the length of the nanowires, it is easy to show that the nanowire array electrode had 10 cm^2 of Pt area per cm^2 of substrate electrode area. The value for a commercial Pt–Ru black (Johnson Matthey, Hispec 6000) is 2.1 cm^2 Pt/cm^2 thin-film electrode [19]. The morphologies of the Pt nanowires and Pt nanowire array electrode are the same as the Pt–Ru nanowires and Pt–Ru nanowire array electrode, so they are not shown here.

3.3. XRD analysis of Pt and Pt–Ru nanowire array electrodes

Fig. 4 shows the XRD patterns of the as-prepared Pt and Pt–Ru nanowire array electrodes. In the samples, only the reflections corresponding to the planes (1 1 1), (2 0 0), (2 2 0), and (3 1 1), characteristic of the face-centered cubic (fcc) structure of Pt are present. With the introduction of Ru into the fcc structure of Pt, the Pt refections are shifted to higher 2θ, which is characteristic of a contraction of the lattice. No peaks characteristic of Ru or Ru oxides were detected, but their presence cannot be dismissed because they may be present in a very small amount or even in an amorphous form.

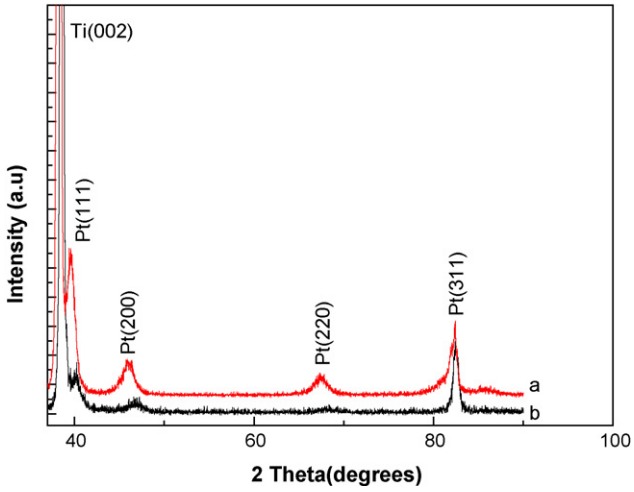

Fig. 4. XRD patterns of Pt (a) and Pt–Ru (b) nanowire array electrodes.

3.4. EDS analysis of the Pt–Ru nanowire array electrode

EDS analysis of the Pt–Ru nanowire array electrode in Fig. 5 confirms a nearly 9:1 atomic ratio of Pt to Ru. The study of Hubert A. Gasteiger et al. [30] concluded that the high catalytic activity of Pt–Ru alloys in the electro-oxidation of methanol derives from the bifunctional character of the alloy surface: the adsorption of methanol on Pt ensembles and the oxidative

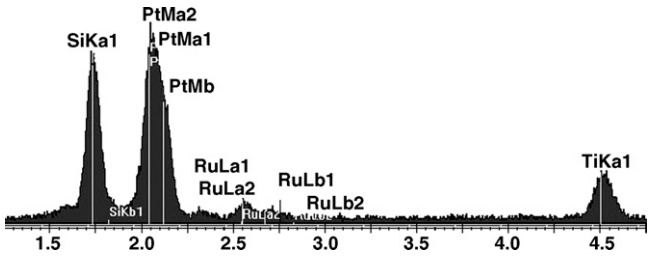

Fig. 5. EDS pattern of Pt–Ru nanowire array electrode.

removal of methanol dehydrogenation fragments by oxygen-like species adsorbed onto adjacent Ru atoms. A statistical model is presented which predicts rather precisely the optimum alloy composition of ≈10 at.%.

3.5. Electrochemical properties of Pt and Pt–Ru nanowire array electrodes

Fig. 6 shows the CVs for methanol oxidation at Pt (Fig. 6(a)) and Pt–Ru (Fig. 6(b)) nanowire array electrode surface in 0.5 M sulfuric acid containing 0.5 M methanol solution. We can find that the CV of methanol oxidation on Pt–Ru nanowire array electrode is very similar to that of a Pt nanowire array electrode. The shape of the CV curves and the peak potential (E_p) are in accord with other work [31]. In the forward scan, methanol oxidation produced a prominent symmetric anodic peak, the peak potential of 0.73 V for Pt and of 0.6 V for Pt–Ru nanowire array electrode. In the reverse scan, there was an anodic peak detected on both Pt and Pt–Ru nanowire array electrode, Goodenough et al. and Lijuan Zhang et al. attributed this anodic peak in the reverse scan to the removal of the incompletely oxidized carbonaceous species formed in the forward scan [32,33]. Hence the ratio of the forward anodic peak current density (I_f) to the reverse anodic peak current density (I_b), I_f/I_b, can be used to describe the catalyst tolerance to carbonaceous species accumulation. A low I_f/I_b ratio indicates poor oxidation of methanol to carbon dioxide during the anodic scan and excessive accumulation of carbonaceous residues on the nanowire array electrode surface. A high I_f/I_b ratio shows the reverse case.

From qualitative analysis of these voltammetric profiles, three aspects are immediately evident. First, at the Pt–Ru nanowire array electrode surface, the peak potential for methanol oxidation is shifted negatively by over 130 mV. Second, the current density at the Pt–Ru nanowire array electrode is higher than that for the Pt nanowire array electrode. Thirdly, the I_f/I_b ratio of 1.28 for Pt–Ru nanowire array electrode is higher than that of Pt ($I_f/I_b = 1.08$), which indicated more intermediate carbonaceous species are oxidized to carbon dioxide in the forward scan on Pt–Ru nanowire array electrode surface than on Pt nanowire array electrode surface.

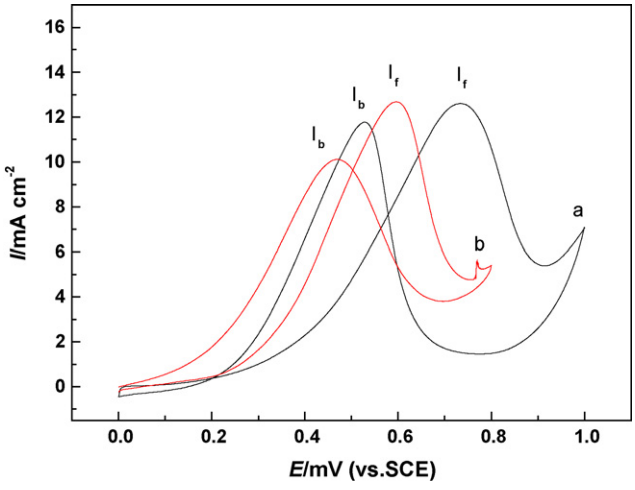

Fig. 6. Cyclic voltammograms of 0.5 M CH_3OH in 0.5 M H_2SO_4 at Pt nanowire array electrode (a) and Pt–Ru nanowire array electrode (b). Scan rate: 50 mV s^{-1}.

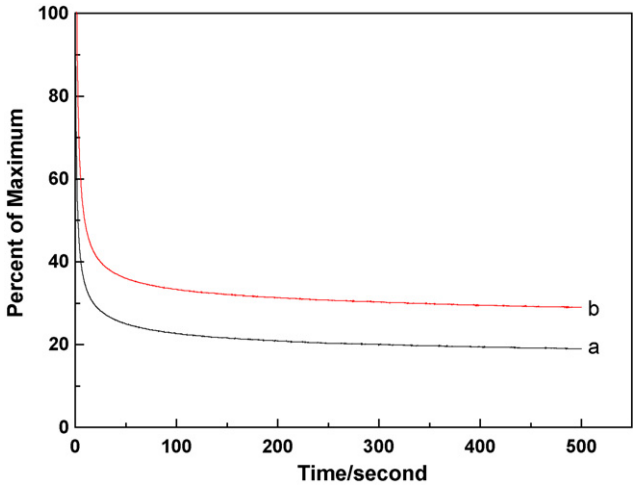

Fig. 7. Chronoamperograms of 0.5 M CH_3OH in 0.5 M H_2SO_4 at Pt nanowire array electrode (a) and Pt–Ru nanowire array electrode (b).

The chronoamperograms (CA) of Pt and Pt–Ru nanowire array electrodes at 0.5 V are compared in Fig. 7. With the potential fixed at 0.5 V, methanol was continuously oxidized on the electrodes and the tenacious reaction intermediates such as CO_{ads} would begin to accumulate if the kinetics of the removal reaction could not keep pace with that of methanol oxidation. A more gradual decay of the current density with time is nevertheless an indication of improved CO resistance. The oxidation current density decreases to 30% of its initial value after 500 s for the Pt–Ru nanowire array electrode as shown in Fig. 7, whereas the corresponding decay for the Pt nanowire array electrode was more severe, at 18%. The improved CO-tolerance of the Pt–Ru nanowire array electrode can be explained by a bifunctional mechanism [34,35] in which the reaction between strongly bound Pt_3CO species and OH_{ads} on neighbouring Ru sites contribute to the major removal mechanism. This is consistent with the work of Jianhuang Zeng and Jim Yang Lee [36].

4. Conclusions

A new method has been introduced to construct catalysts for methanol electro-oxidation using an AAO template on a Ti/Si substrate. The structure and electrocatalytic properties of a Pt–Ru nanowire array electrode have been investigated (the optimum alloy composition was ≈ 10 at.%). The nanowire array electrodes had a high electrode area, and there was almost no waste of Pt and Ru in contrast to the traditional method because of electrochemical method used to construct the electrodes. AAO/Ti/Si may be a good candidate for making electrodes for portable fuel cell power sources. From the C/V and the C/A data, we can conclude that the Pt–Ru nanowire array electrode shows better electrocatalytic activity and stability for methanol oxidation than the Pt nanowire array electrode.

Acknowledgment

This work is supported by the National Natural Science Foundation of China (NNSFC60471014).

References

[1] C.K. Dyer, J. Power Sources 106 (2002) 31.
[2] C.Y. Chen, P. Yang, J. Power Sources 123 (2003) 37.
[3] F. Vigier, C. Coutanceau, A. Perrard, E.M. Belgsir, C. Lamy, J. Appl. Electrochem. 34 (2004) 439.
[4] C. Lamy, S. Rousseau, E.M. Belgsir, C. Coutanceau, J.-M. Le′ger, Electrochim. Acta 49 (2004) 3901.
[5] E.V. Spinace′, A.O. Neto, M. Linardi, J. Power Sources 129 (2004) 121.
[6] L.H. Jiang, Zh.H. Zhou, W.Z. Li, W.J. Zhou, S.Q. Song, H.Q. Li, G.Q. Sun, Q. Xin, Energy Fuel. 18 (2004) 866.
[7] H. Wang, Z. Jusys, R.J. Behm, J. Phys. Chem. B 108 (2004) 19413.
[8] S.R. Narayanan, H. Frank, B. Jeffries-Nakamura, M. Smart, W. Chun, G. Halpert, J. Kosek, C. Cropley, in: S. Gottesfeld, G. Halpert, A. Landgrebe (Eds.), Proton Conducting Membrane Fuel Cells I, PV 95–23, The Electrochemical Society Proceedings Series, Pennington, NJ, 1995, p. 278.
[9] X. Ren, T.E. Springer, S. Gottesfeld, J. Electrochem. Soc. 147 (2000) 92.
[10] A.S. Arico, S. Srinivasan, V. Antonucci, Fuel Cells 1 (2001) 133.
[11] A.K. Shukla, C.L. Jackson, K. Scott, R.K. Raman, Electrochim. Acta 47 (2002) 3401.
[12] D.J. Guo, H.L. Li, J. Electroanal. Chem. 573 (2004) 197.
[13] C.S. Kelly, G.A. Deluga, W.H. Smyrl, Electrochem, Solid State Lett. 3 (2000) 407.
[14] J. Yu, P. Cheng, Z. Ma, B. Yi, J. Power Sources 124 (2003) 40.
[15] M. Hayase, T. Kawase, T. Hatsuzawa, Electrochem, Solid State Lett. 7 (2004) A231.
[16] S. Motokawa, M. Mohamedi, T. Momma, S. Shoji, T. Osaka, Electrochem. Commun. 6 (2004) 562.
[17] K.-B. Min, S. Tanaka, M. Esashi, Electrochemistry 70 (2002) 924.
[18] S. Onoue, H. Tanaka, K. Hoshino, K. Matsumoto, I. Shimoyama, Proceedings of the Transducers_05, 2005, p. 1296.
[19] W.C. Choi, S.I. Woo, J. Power Sources 124 (2003) 420.
[20] F. Liu, J.Y. Lee, W. Zhou, J. Phys. Chem. B 108 (2004) 17959.
[21] R.E. Ricker, A.E. Miller, D.F. Yue, G. Banerjee, J. Electron. Mater. 25 (1996) 1585.
[22] M. Saito, M. Kirihara, T. Taniguchi, M. Miyagi, Appl. Phys. Lett. 55 (1989) 607.
[23] S. Kawai, R. Ueda, J. Electrochem. Soc. 122 (1975) 32.
[24] D. AlMawiawi, N. Coombs, M. Moskovits, J. Appl. Phys. 70 (1991) 4421.
[25] S. Tan, M. Reed, H. Han, R. Boudreau, Proceedings of the IEEE Micro Electro Mechanical Systems, vol. 29, Amsterdam, The Netherlands, 1995, p. 267.
[26] P. Hoyer, N. Baba, H. Masuda, Appl. Phys. Lett. 66 (1995) 2700.
[27] M. Nakao, S. Oku, T. Tamamura, K. Yasui, H. Masuda, Jpn. J. Appl. Phys., Part 1 38 (1999) 1052.
[28] Y.F. Mei, X.L. Wu, X.F. Shao, G.S. Huang, G.G. Siu, Phys. Lett. A 309 (2003) 109.
[29] M.S. Sander, L.S. Tan, Adv. Funct. Mater. 13 (2003) 393.
[30] A. Hubert, Gasteiger, M. Nenad, N. Philip Jr. Ross, J. Elton, J. Phys. Chem. 97 (1993) 12020.
[31] K. Yahikozawa, Y. Fujii, Y. Mitlsuda, K. Nishimura, Y. Takasu, Electrochim. Acta 36 (1991) 973.
[32] R. Manohara, J.B. Goodenough, J. Mater. Chem. 2 (1992) 875.
[33] L. Zhang, D. Xia, Appl. Surf. Sci. 252 (2006) 2191.
[34] N.M. Markovic, H.A. Gasteiger, P.N. Ross, X. Jiang, I. Villgas, M.J. Weaver, Electrochim. Acta 141 (1995) 91.
[35] K. Wang, H.A. Gasteiger, N.M. Markovic, P.N. Ross Jr., Electrochim. Acta 41 (1996) 2587.
[36] J. Zeng, J.Y. Lee, J. Power Sources 140 (2005) 268.